Facile fabrication of high performance nanofiltration membranes for recovery of triazine-based chemicals used for H_2S scavenging

Khalil, Alaa; Montesantos, Nikolaos; Maschietti, Marco; Muff, Jens

Published in:
Journal of Environmental Chemical Engineering

DOI (link to publication from Publisher):
10.1016/j.jece.2022.108735

Publication date:
2022

Document Version
Publisher's PDF, also known as Version of record

Journal of Environmental Chemical Engineering 10 (2022) 108735

Contents lists available at ScienceDirect

Journal of Environmental Chemical Engineering

journal homepage: www.elsevier.com/locate/jece

Facile fabrication of high performance nanofiltration membranes for recovery of triazine-based chemicals used for H_2S scavenging

Alaa Khalil [a,b,*], Nikolaos Montesantos [a], Marco Maschietti [a], Jens Muff [a,b]

[a] Aalborg University, Department of Chemistry and Bioscience, Section of Chemical Science and Engineering, 6700 Esbjerg, Denmark
[b] Aalborg University, Center for Membrane Technology, Frederik Bajers Vej 7H, 9220 Aalborg Ø, Denmark

ARTICLE INFO

Keywords:
Thin-film composite
Nanofiltration
Triazine-based H_2S scavenger
Spent and unspent scavengers

ABSTRACT

The synthesis of tailormade thin-film composite (TFC) nanofiltration (NF) membranes produced by interfacial polymerization is presented for the separation of unspent (MEA-triazine) and spent (DTZ) H_2S scavengers obtained from an oil and gas wastewater from an offshore installation in the North Sea. The physicochemical properties, thermal stability, and hydrophilicity of the synthesized TFC membranes were investigated using SEM, FTIR, XRD, TGA, and contact angle. Filtration layer thicknesses from 25 to 400 μm were investigated and the optimal value (100 μm) was determined, based on the efficiency in the separation and the water permeability. Operating at 50% permeate recovery, rejections for MEA-triazine and monoethanolamine of 62% and 82%, respectively, were obtained, with zero rejection for DTZ. In 24 h batch recirculation tests, the water permeability remained stable at 6 L/(m^2·h·bar), indicating insignificant fouling with 13 times higher compared to the 0.45 L/(m^2·h·bar) achieved by the commercial NF270 membrane under comparable conditions. The results indicate that the NF of mixtures of spent/unspent H_2S scavengers using tailored membranes is a promising strategy for recovering MEA-triazine, thus reducing costs for offshore oil and gas operators, while reducing the environmental impact associated to the discharge of this wastewater.

1. Introduction

The oil and gas industry has long been challenged by the need of removing hydrogen sulfide (H_2S) from the hydrocarbon production streams. H_2S is a colorless, highly corrosive, and combustible gas with high toxicity even at the low concentration levels commonly observed in natural gas and crude oil [1]. To increase the lifespan of facilities and comply with environmental and safety regulations, the content of H_2S must often be reduced in upstream operations, i.e., before the hydrocarbons are transported or stored. In the case of offshore oil and gas production, H_2S is typically removed by direct injection of chemicals, called H_2S scavengers, into the production streams. The scavengers convert H_2S into by far less hazardous and corrosive species [2,3].

1,3,5-Hexahydrotriazines are the most common H_2S scavengers used nowadays, with a recent trend towards water-soluble species [4]. More specifically, the water-soluble species 1,3,5-tri(2-hydroxyethyl)hexahydro-S-triazine (HET), also known as MEA-triazine in oil and gas industry, is by far the most popular H_2S scavenger accounting for more than 80% of the oilfield market due to very favorable scavenging kinetics [5]. Concerning the application of HET to treat natural gas, a basic aqueous solution of the scavenger is injected and dispersed into the gas stream, leading to the H_2S absorption and conversion into organics containing nitrogen and sulfur [6]. The two nitrogen atoms in HET are replaced in two sequential steps with the sulfur atoms from H_2S, generating monoethanolamine (MEA) in each step and 5-(2-hydroxyethyl)hexahydro-1,3,5-dithiazine (DTZ) in the second step [7,8]. HET is generally utilized in large stoichiometric excess to increase the rate of the H_2S removal and assure that the concentration of H_2S in the gas stream is reduced below the maximum allowed limits in the given contact times. Downstream of the separation of the gas stream from the scavenging solution, a wastewater containing unreacted HET, MEA and DTZ is therefore obtained. The spent and unspent scavenger (SUS) wastewater is problematic to handle due to its fouling and scaling propensity caused by its alkaline pH and DTZ polymerization [3]. The SUS stream frequently ends up in the water discharge from the platform due to lack of feasible alternatives [2]. Even though it is a small-size stream, compared to the total produced water discharge, it contributes significantly to the environmental impact of offshore oil and gas production to the marine environment. It is worth mentioning that triazines find use as pesticides, while MEA is classified by the European Chemicals Agency (ECHA) as

* Corresponding author at: Aalborg University, Department of Chemistry and Bioscience, Section of Chemical Science and Engineering, 6700 Esbjerg, Denmark.
E-mail address: amaak@bio.aau.dk (A. Khalil).

https://doi.org/10.1016/j.jece.2022.108735
Received 30 May 2022; Received in revised form 8 September 2022; Accepted 7 October 2022
Available online 12 October 2022

harmful to marine life with long-term impacts [9]. Therefore, it would be beneficial to treat the SUS wastewater before discharge to recover the unreacted HET and the produced MEA, thus reducing the environmental impact.

Membrane technology among other water treatment processes might be considered as a possible choice for the treatment of SUS solution due to its modular structure, which allows adapting it to the existing offshore facility due to the small size of the SUS wastewater stream [10,11]. Furthermore, it provides benefits in terms of low environmental impact because membranes do not require the use of chemical additives. In a recent work, it has been shown that nanofiltration (NF) with the commercially available FilmTec™ NF270, which is a thin-film composite polyamide membrane, could separate HET (rejection 71%) and MEA (rejection 50%) from DTZ (zero rejection) in a lab-scale study carried out on a real offshore SUS feed. This work has demonstrated the potential for preventing discharge of unreacted HET and MEA into the sea, while opening for the opportunity of reusing the unreacted HET, thus offering environmental as well as economic benefits for the operators [12]. To realize the potential, it would be desirable to improve the mass balance of the selective HET recovery by increasing the HET rejection by the NF membrane, while still allowing DTZ to pass through and increasing the membrane permeability. This calls for tailor-made NF membranes for this particular application, which has not previously been considered on a commercial scale. Membrane separation performance depends on the differences in mass transfer of target molecules through the membrane. Transport distance (thickness) through the membrane is an important factor for mass transport, and in this work, we investigate how varying the thickness of the middle layer of a thin-film composite (TFC) membrane influence the separation performance. During membrane synthesis, varying the thickness of this layer is rather facile and has not been well explored in published research, compared to the more complex process of varying the dense top layer. TFC membranes are composed of an ultrathin polymeric selective layer and a porous substrate. In general, TFC membranes offer many advantages such as low operating pressure, high retention toward organic molecules, high flux, and low maintenance costs compared to traditional separation processes [13]. For TFC membranes, interfacial polymerization (IP) is utilized to produce polyamide (PA) filtration layers on top of typically polysulfone support to achieve a reverse osmosis (RO) and nanofiltration (NF) membrane suitable for filtration of organic and aqueous liquids. The active PA layer is around 10–200 nm thick, and the resultant membranes have in the literature shown permeabilities that increase with decreased PA thickness, two orders of magnitude above commercial TFC membranes while maintaining the rejection of the target contaminant [14]. Different materials have also been used to improve the separation performance and anti-fouling capabilities of thin-film polyamide membranes [15–17]. Recently, dopamine (DA) has been employed for the fabrication of highly-efficient membranes. Dopamine converts to polydopamine (PDA) through self-polymerization in an alkaline environment in the presence of oxygen. In fact, polydopamine (PDA) functions as an adaptable organic nanomaterial capable of homogeneous dispersion into the polymer matrix due to its superior properties such as being tightly adherent and highly hydrophilic because of the inclusion of catechol, quinone, imine and amine groups. Polysulfone (PSF) has been widely utilized as a membrane material for water treatment due to its high permeability, hydrophilicity, as well as mechanical, thermal, and chemical stability [18]. Polyvinylpyrrolidone (PVP) has been used as a pore-forming agent which can modify the structure of membranes such as pore formation and interconnectivity, resulting in improved separation performance [19,20]. A first approach to optimize a TFC membrane towards a specific application is to change the thickness of the filtration layer as demonstrated in previous works [21–25].

In this work, we demonstrate a facile fabrication of a TFC membrane with different PSF layer thickness by using interfacial polymerization with the aim of selective rejection of HET from SUS wastewater. Chemical structure, morphology, thermal stability, and physicochemical properties such as surface charge, and hydrophilicity of the synthesized TFC membrane surface were investigated to verify the stability and integrity of the prepared membrane. The performance of the synthesized TFC membrane was investigated for the treatment of a sample of SUS wastewater obtained from an offshore oil and gas installation in the North Sea. In addition, the nanofiltration experiments were also applied to single solute solutions (HET, MEA, and DTZ) to elucidate the interactions of these species with the membrane. Furthermore, the effect of the PSF layer thickness was also investigated in order to check the separation performance with the modification applied and the results were compared to the performance of the commercial NF270 membrane. Measurements of water permeability and 24 h filtration studies were also conducted to examine the fouling propensity of the SUS wastewater on the synthesized TFC membranes.

2. Experimental

2.1. Materials

Polyethylene terephthalate non-woven support fabrics (PET, Novatexx 2413) were purchased from Freudenberg Group (Germany). Polysulfone pellets (PSF, MW: 35,000 g·mol^{-1}, Sigma-Aldrich, Denmark), polyvinylpyrrolidone (PVP, MW: 35,000 g·mol^{-1}, Sigma-Aldrich, Denmark), and N-methyl-2-pyrrolidone (NMP, Sigma-Aldrich, Denmark) were used to prepare a polysulfone porous substrate. m-Phenylenediamine (MPD, 99 %, Sigma-Aldrich, Denmark), dopamine hydrochloride (DA, Sigma-Aldrich, USA), trimesoyl chloride (TMC, 98 %, Sigma-Aldrich, Denmark), and n-hexane, (VWR, Redmond, WA) were used for interfacial polymerization.

The SUS solution was provided from an offshore oil and gas production platform in the North Sea. The sample was collected offshore, downstream of the separation from the gas, depressurized to atmospheric pressure, and delivered to our laboratory where it was stored at 4 °C. The pH and conductivity of the SUS solution were measured using a pH meter (Metrohm, 913) and a conductometer (Metrohm, 912), respectively. The viscosity of the SUS solution was measured using a cone and plate viscometer (Brookfield, CAP 2000). The physical and chemical properties of the SUS solution are shown in Table 1. 1,3,5-tri(2-hydroxyethyl)hexahydro-*S*-triazine (HET, ≥95 %, Santa Cruz Biotechnology), monoethanolamine (MEA, ≥99 %, Acros Organics), and 5-(2-hydroxyethyl)hexahydro-1,3,5-dithiazine (DTZ, ≥98 %, Toronto Research Chemicals) were used to prepare single solute solutions and as external standards for the calibrations. Methyl heptadecanoate (MHD, ≥99.0 %, Sigma-Aldrich) and 1-Propanol (≥99.5%, VWR) were used as an internal standard for GC–MS and GC-FID, respectively. Dichloromethane (DCM, ≥99.8 %, VWR) was used as a liquid-liquid extraction solvent.

2.2. Preparation of thin film nanocomposite membranes

The PSF powder was dried overnight before usage and a certain amount of PSF and PVP were added to NMP as a solvent. The mixture was kept under stirring overnight at 50 °C until a homogeneous solution

Table 1
Physical and chemical properties of SUS solution.

Physical properties		Chemical properties	
Density (kg/m^3)	1024 (22 °C)	TOC (g/L)	98 ± 5
Viscosity (cP)	2.6 (25 °C)	Triazine (HET, g/L)	140 ± 15
Conductivity (mS/cm)	10.3 (22 °C)	Monoethanolamine (MEA, g/L)	69 ± 12
		Dithiazine (DTZ, g/L)	25 ± 3
		pH	10.2

was obtained. The casting solution was subsequently left without stirring to remove air bubbles. The solution was cast onto the PET nonwoven fabrics using a doctor blade (TQC Sheen, The Netherlands) with thickness values in the range 25–400 μm and a casting velocity of 5 mm/s. After casting, the obtained membranes were soaked in a coagulation bath at room temperature for 24 h. The fabricated membranes were washed and stored in deionized water before the application of IP. The polysulfone membranes were immersed in an aqueous solution of MPD (2 wt%) and DA (0.1 wt%) for 2 min, and the remaining solution was wiped away from the membrane surface. Subsequently, IP was carried out by transferring a n-hexane solution of TMC (0.1 wt%) into the membrane surface for 1 min. The TFC membranes were heat-treated in an oven at 60 °C for 20 min and then stored in deionized water prior to use (Fig. 1). The synthesized (PET+PSF+PA) membranes were denoted by TFC and the synthesized (PET+PSF) membranes by PSF.

2.3. Membrane characterization

The morphology of the surface of the membranes and their cross-sections were characterized by scanning electron microscope (SEM, FEI Quanta 650 F). The membranes were submerged in liquid nitrogen for 3 min and then broken to examine the cross-section morphology. Fourier Transform infrared spectroscopy (FTIR, Thermo Scientific, Nicole iS5, US) was used to examine the chemical structures of the membrane surface and X-ray diffraction (XRD, Panalytical Ltd, Aeris, UK) was used to evaluate the composition of the membranes. Thermogravimetric analysis in a TG/differential thermogravimetry (DTG) was used to determine the thermal stability of the prepared membranes at a heating rate of 10 °C/min in N_2 using a TGA-550 equipment (TA Instruments, US). Contact angle (CA) at the interface between water and the membrane surface was measured with a drop shape analyzer (KRÜSS DSA 100, Germany) using the sessile drop method to assess its hydrophilicity. MilliQ water (2 μL) was used to generate the droplets to be contacted with the membrane surface at room temperature. For each membrane, the CA values presented in this work are the average of five measurements taken at various places. The surface charge of the membrane was measured by a SurPASS electrokinetic analyzer (Anton Paar GmbH, Graz, Austria) using 1 mM KCl aqueous solution as an electrolyte solution and a 100 ± 2 μm gap between the membranes (Fig. S1). The influence of pH on the zeta potential was investigated using automatic titration with 0.1 M HCl and 0.1 M NaOH.

2.4. Analytical characterization

HET and MEA were measured using a GC-FID (PerkinElmer Clarus 690, USA). DTZ was quantified via liquid-liquid extraction procedure with DCM using gas chromatography coupled with mass spectrometry (GC–MS, PerkinElmer Clarus 680 GC, PerkinElmer Clarus SQ 8 T MS, USA). The concentrations of HET, MEA, and DTZ were determined by means of the external standard method. Internal standards were also used expressing the response of each species relative to the respective internal standard. The analysis of each sample was repeated three times with relative standard deviation (RSD) less than 5%. A multi-N/C 2100 TOC analyzer was used to quantify total organic carbon (TOC). All the measurements were repeated three times, resulting in RSD values that were always less than 1% and the averages were provided. More details about the SUS solution analysis are reported elsewhere [2].

2.5. Membrane filtration protocol

The membrane performance was evaluated using a cross-flow filtration system (FT17–50, Armfield, UK) comprising a membrane cell, a feed pump, a pressure gauge (0–40 bar), a thermometer, an electronic balance, and a feed vessel equipped with a thermostatic jacket connected to a heating/cooling unit to adjust the temperature as shown in Fig. 2. The system is connected to a computer for data acquisition. The volume of the feed vessel is 1 L with a membrane coupon diameter of 90 mm (effective surface area of 63.6 cm^2).

For each experiment, all the membranes were pre-compacted by deionized water for 1 h at a transmembrane pressure (TMP) of 10 bar until the permeate flux was constant. Membrane pure water flux was measured with five different TMP values in the range 1–10 bar at 25 °C. Concerning the experiments with SUS and single-solute solutions, 500 mL of SUS wastewater was circulated through the system at approximately zero-gauge pressure for 30 min to allow the membrane surface to saturate. After that, the feed solution was filtrated at a TMP of 1 bar for the synthesized TFC membrane due to the high permeability of the membrane and 30 bar for the commercial NF270 membrane due to the low permeability and for the comparison to our previous work, and at 40 °C with 2.5 m/s cross-flow velocity and a 100 L/h feed flow rate. The experiment was stopped when a permeate mass of 50% of the mass of the feed was collected. The membrane permeability and the rejection of individual species, as well as the TOC rejection, were measured. The permeability (P_m) and the rejections (R) of the TFC membranes were calculated as follows:

$$P_m = \frac{V_P}{A\Delta Pt} \quad (1)$$

$$R = 1 - \frac{C_P}{½(C_F + C_R)} \quad (2)$$

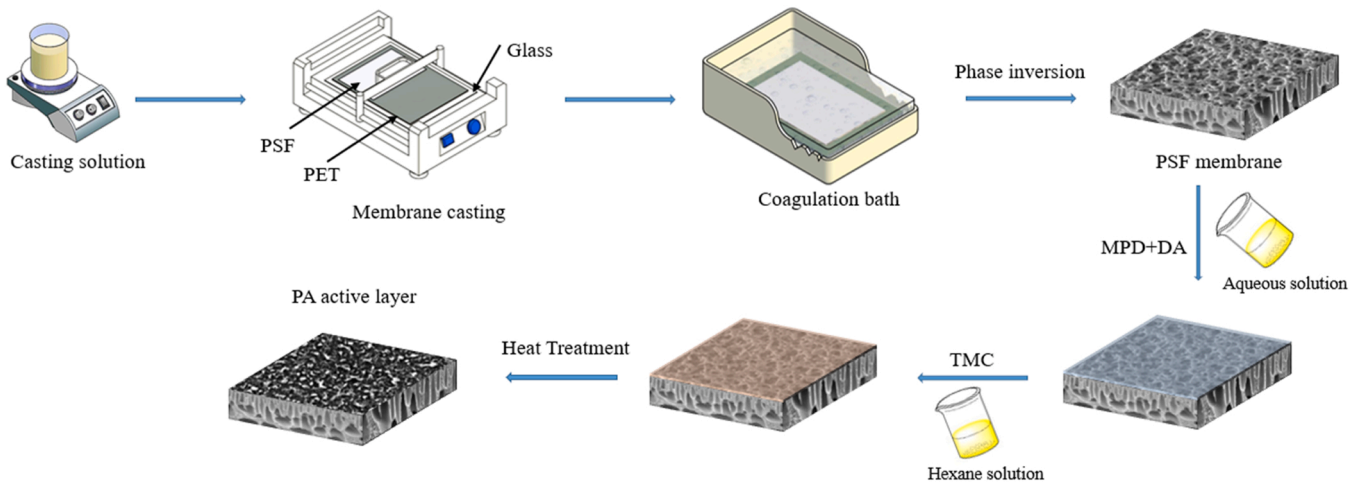

Fig. 1. Schematic illustration of the fabrication of a TFC membrane.

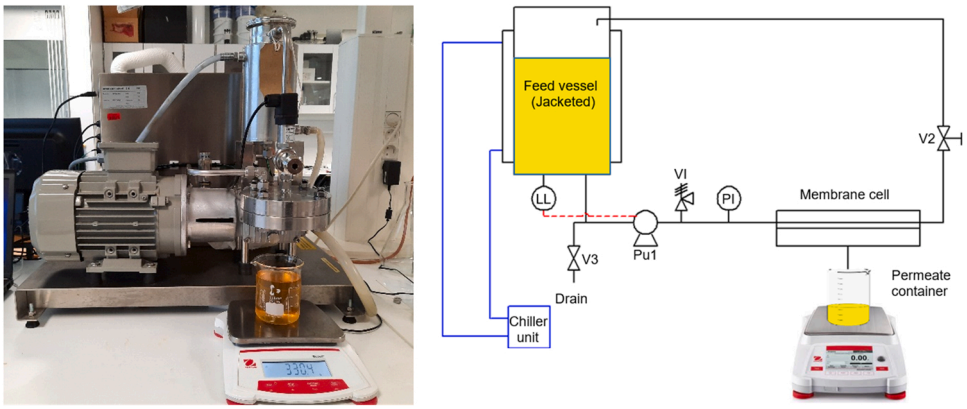

Fig. 2. Photograph and schematic of the cross-flow filtration system.

$$TOC \quad rejection = 1 - \frac{TOC_p}{½(TOC_F + TOC_R)} \tag{3}$$

where V_p is the permeate volume, A is the effective filtration area, ΔP is the transmembrane pressure and t is the filtration time. C_F, C_P, and C_R are the concentrations of the species under consideration in the feed, permeate and retentate solution, respectively. Analogously, TOC_F, TOC_P, and TOC_R are the TOC values of the feed, permeate and retentate solution.

Membrane fouling is the deposition and accumulation of unwanted materials on membrane surfaces, which causes a decrease in membrane flux, a decrease in membrane performance, as well as high transmembrane pressure (TMP), and high maintenance cost. Therefore, it should be minimized as it causes challenges in large-scale applications. In this regard, 1 L SUS wastewater was used to investigate the fouling propensity of the synthesized TFC and NF270 membranes during 24 h at TMP values of 1 bar and 30 bar, respectively. Also, in this type of experiments, the membranes were pre-compacted at TMP of 10 bar with deionized water for at least 1 h and the SUS wastewater was circulated through the system at approximately zero gauge pressure for 30 min. The permeate was returned to the feed vessel to keep the feed concentration constant in order to approximate a steady-state filtration process. Samples were collected every 4 h from both the feed and the permeate to calculate the rejection of individual SUS species and TOC, as well as the permeability over time.

3. Results and discussion

3.1. Membrane Characterization

Fig. 3 shows the surface morphology and cross section

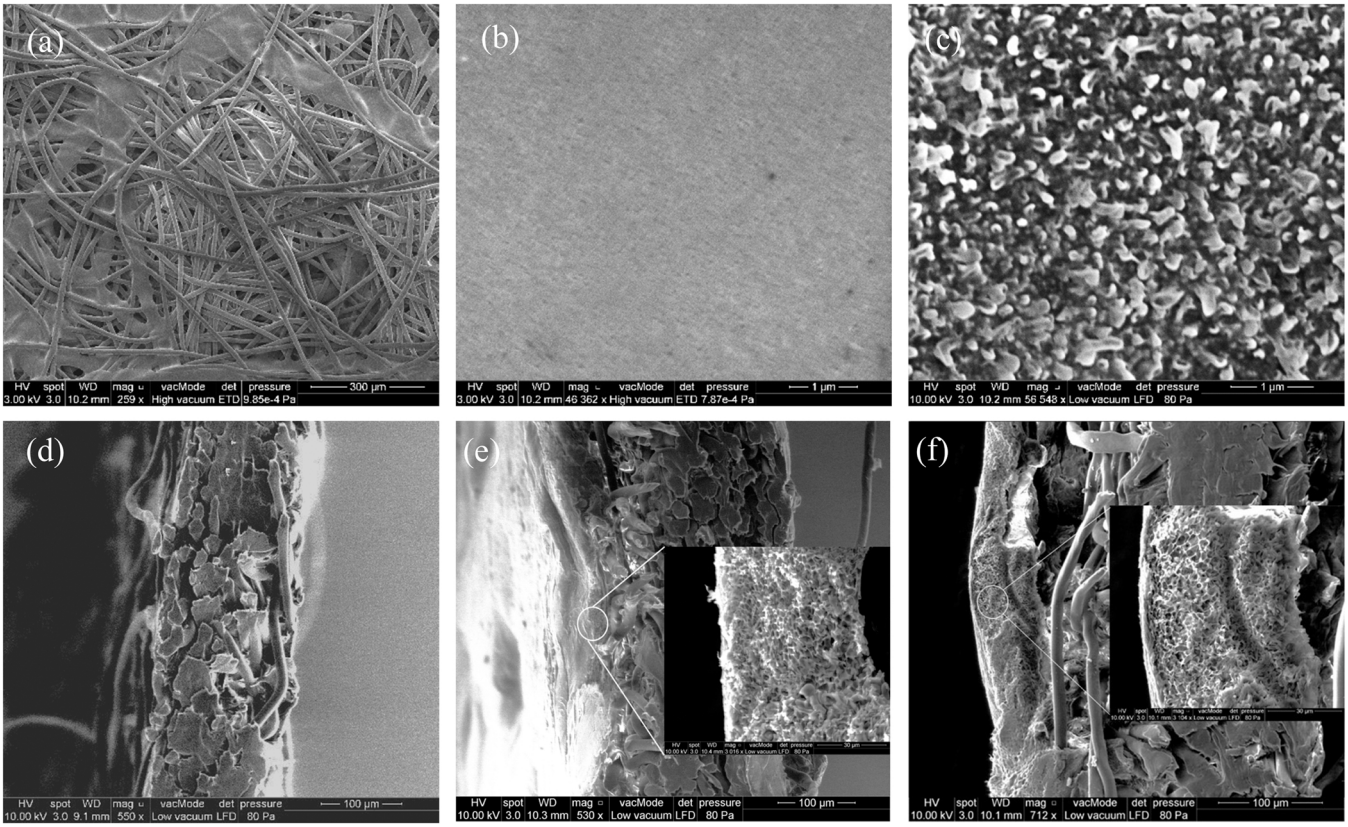

Fig. 3. SEM image of surface morphology and cross section of a,d) PET, b,e) PSF and c,f) TFC membranes.

microstructure of the PET substrate, PSF, and TFC membranes. The PET substrate is highly porous as shown in Fig. 3a. The surface morphology of the PSF and the synthesized TFC membrane has no evident pores or defects (Fig. 3b and c). The top surface of the PSF membrane (Fig. 3b) has a smooth and flat surface with no protrusions. On the other hand, the synthesized TFC membrane has granular-like structures without distinct cavities on the top surface, which evidences the formation of PA layers on the PSF substrate (Fig. 3c). The cross-sectional SEM images of the synthesized TFC membrane (Fig. 3f) show a sponge-like pore structure that initiates just below the top surface of the porous PSF support, which is uniformly coated with a thin layer of polyamide. The polysulfone substrate layer and the polyamide skin layer in the membrane are evident in the cross-section images (e and f), with a 100–250 nm skin layer. The sponge-like micro-voids extend from the PSF surface of the substrate all the way through the layer.

A hydrophilic surface is an important characteristic of a membrane to promote high permeability and decrease fouling propensity. The hydrophilicity of the membranes was determined using contact angle analysis, as illustrated in Fig. 4a. Fig. 4a depicts the change in contact angle during the various stages of membrane preparation. The average contact angle of the hydrophobic PET membrane was 104°, while it was 73° for the PSF membrane, whereas the synthesized TFC membrane had a much lower contact angle of 51°. As a term of comparison, the commercial NF270 membrane showed a CA of 54°. These data indicate the increased hydrophilicity of the synthesized TFC membrane, comparable with the contact angles published in the literature for same type of membranes [26]. This result is attributed to the permeation of diamine into the pores of the PSF membrane layer which connects to the pore wall via self-polymerization during the TFC formation process, increasing their hydrophilicity compared to the pure PSF layer [27]. In addition, the synthesized TFC membrane is more hydrophilic than commercial NF270 due to the presence of DA, which has hydrophilic hydroxyl and amine groups, leading to the lowest contact angle, reducing the permeation resistance, and consequently the highest wettability of the surface, as previously observed in the literature.

Thermogravimetric analysis was used to investigate the thermal stability of the PET substrate, as well as the PSF and TFC membranes as shown in Fig. 4b. The PET substrate shows a single degradation stage at 345–516 °C with a weight loss of 86.4%. The DTG curve shows the maximum decomposition rate at 414 °C, which corresponds to the decomposition of cyclic oligomers and the release of acetaldehyde groups and anhydride oligomers [28]. For the PSF membrane, the weight loss below 200 °C corresponds to water and solvent losses, while the weight loss of 80.6% in the temperature range 340–500 °C is ascribed to the thermal decomposition of the polysulfone layer with maximum weight loss observed at 419 °C [29]. The TGA curve of the synthesized TFC membrane shows three different stages of weight losses: (i) a first stage in the temperature range of 345–430 °C, which is caused by the thermal decomposition of the PET substrate and accounts for a weight loss of 66.7 %; (ii) a second stage in the temperature range of 445–550 °C, which is due to the degradation of the polyamide layer and accounts for a weight loss of 13.2%; and (iii) a third stage starting at 560 °C, which is associated to the degradation of the polysulfone layer [30].

The appropriate infrared absorption bands of the PET substrate, as well as of the PSF and TFC membranes, are shown in Fig. 5. For PET, the stretching vibration at 1711 cm^{-1} indicates the carbonyl bonds (C═O), while the vibration bands at 1408 cm^{-1}, 870 cm^{-1}, and 721 cm^{-1} represent aromatic (C═C), (=C–H) and (C–H) bonds, respectively [31]. In addition, the band at 1340 cm^{-1} is associated to aliphatic (C–H) bonds, while the three strong stretching vibration bands at 1239 cm^{-1}, 1091 cm^{-1}, and 1016 cm^{-1} indicate the presence of an ester bond (C–O). For the FTIR spectrum of the PSF membrane, the absorption bands at 1148 cm^{-1} (O═S═O stretching), 1238 cm^{-1} (C–O–C stretching), 1494 cm^{-1} and 1586 cm^{-1} (C═C aromatic) are characteristic of polysulfone [32]. In addition, the bands at 1020 cm^{-1} and 830 cm^{-1} are for C-H stretching of polysulfone aromatic ring [29]. After the IP reaction, two strong characteristic imide bands appear, which are at 1776 cm^{-1} and 1717 cm^{-1} and correspond to the asymmetric and symmetric stretching mode of C═O (imide I). In addition, the band at 1364 cm^{-1} is assigned to the C–N–C stretching mode (imide II) [33]. Three new peaks at 1543 cm^{-1}, 1610 cm^{-1}, and 1665 cm^{-1} are observed in the TFC membranes, attributed to the N–H bending of amide II in the –CO–NH– group, the aromatic amide ring breathing, and C═O stretching vibration in the amide I bond. These peaks are all associated with the polyamide active layer on the PSF membrane [24]. In addition, the reduction in intensity of the peaks at 1244 cm^{-1} and 1152 cm^{-1} in the TFC membrane spectra reveals the formation of the layer on the polysulfone membrane. Furthermore, the peak intensity at 3100–3700 cm^{-1} is ascribed to N–H and O–H stretching vibrations in polydopamine (PDA), leading to increased membrane hydrophilicity [34]. These characteristics are comparable to previous TFC preparations [35,36].

The crystallinity of PET, PSF, and TFC membrane was investigated using X-ray diffraction as shown in Fig. 5b. The characteristic peaks of the TFC membrane and PET are approximately identical, as seen from the literature [37–40]. The PET and TFC membranes exhibit three diffraction peaks at $2\theta = 17.65°$, 22.81°, and 25.87° corresponding to the reflections from the (010), (110), and (100) planes, which emphasize the semi-crystalline structure of the thin film membrane, whereas the broad peak at $2\theta = 17.5°$ corresponds to the amorphous structure of the PSF membrane [41,42].

3.2. Membrane rejection performance

Pure water permeability tests were performed to investigate the effect of each membrane on the transmembrane flux, which affects the energy required for the process. Permeability values for the NF270 and

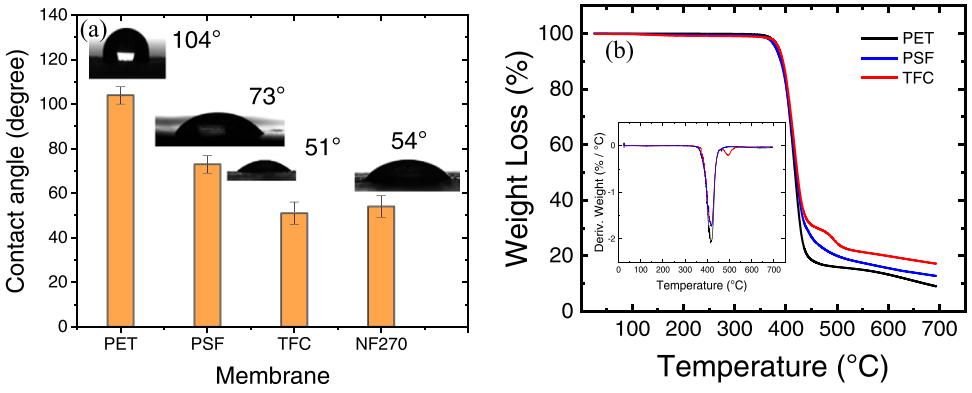

Fig. 4. a) Contact angle of the PET, PSF, TFC and NF270 membrane and b) TGA and DTG of the PET substrate, PSF membrane and TFC membrane.

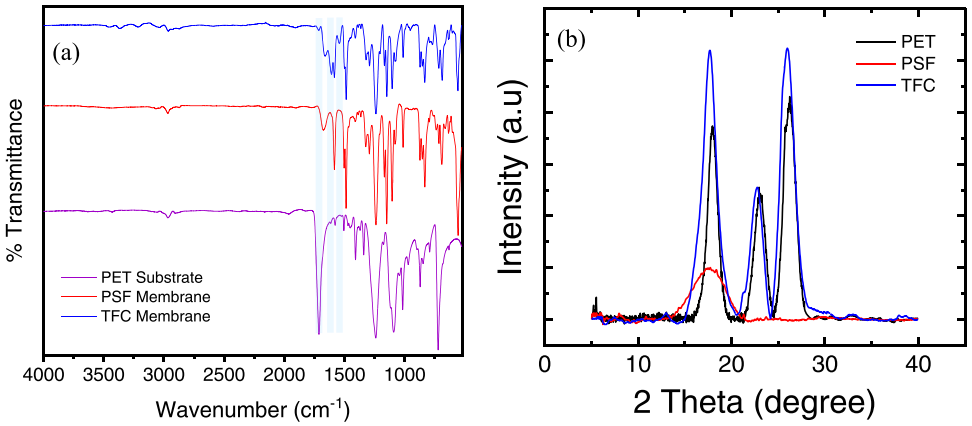

Fig. 5. a) ATR-FTIR images and b) XRD of the PET substrate, PSF membrane and TFC membrane.

the synthesized TFC membrane are shown in Fig. 6. As can be seen, the pure water flux increases linearly with the transmembrane pressure. The permeability of the synthesized TFC membrane was measured to 20 $L{\cdot}m^{-2}{\cdot}h^{-1}{\cdot}bar^{-1}$, which is twice as high as the permeability of the NF270 membrane (10 $L{\cdot}m^{-2}{\cdot}h^{-1}{\cdot}bar^{-1}$). This result is consistent with other TFC membranes reported in the scientific literature, exhibiting higher water permeability compared to typical commercial membranes [43,44]. This is likely due to the differences in the membrane layer thickness.

Membrane thickness is a critical parameter that affects the performance of the membrane as it influences the mass transfer of substances within the membrane wall. Fig. 7 depicts the relationship between average permeability and rejection of HET, MEA, and DTZ from the SUS solution as a function of the membrane thickness, by varying the thickness of the middle PSF layer in the range of 25–400 μm. As can be seen, the rejection of HET and MEA increases as the thickness of the membrane increases up to 100 μm. At higher thickness values, the rejection of HET keeps rather stable at around 60 %. With regard to MEA, the rejection has a maximum of 82 % at 100 μm, while decreasing at higher thicknesses to values in the range of 40–50 %. On the other hand, the rejection of DTZ is close to zero at all conditions. The observation that the HET rejection increases slightly with the PSF layer

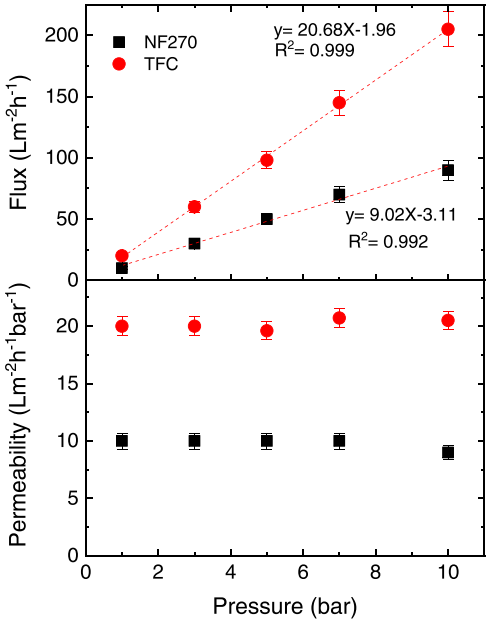

Fig. 6. Pure water flux and permeability as a function of the transmembrane pressure for the NF270 and the synthesized TFC membrane at 25 °C.

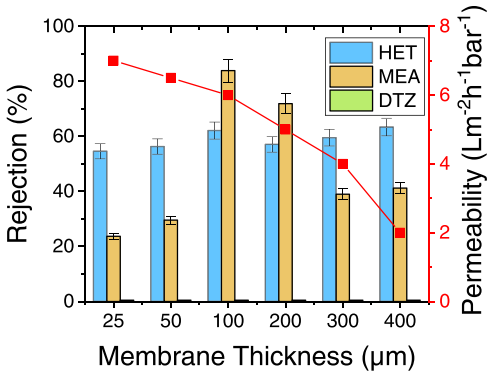

Fig. 7. Effect of membrane thickness on the rejection of HET, MEA and DTZ and permeability of the synthesized membrane (measured at permeate recovery of 50 %).

thickness is of interest and indicate that not only the thickness of the selective PA top layer, which was kept constant in this study, plays a role in separation performance using TFC membranes, but there are interactions between the top layer and the semi-porous PSF middle layer affecting the mass transport through the membrane. Separation is attributed to the different migration/diffusion rates through the non-porous and semi-porous polymeric materials of the membrane, whereas the PET support provides the sufficient strength for the membrane to withstand the applied transmembrane filtration pressure. When the membrane thickness is less than the critical thickness, the rejection of the SUS species increases as the thickness increases. After the membrane thickness exceeds the critical thickness, the rejection of HET, MEA, and DTZ from SUS solution remains almost constant or decreases, as a significant increase in skin layer thickness leads to a reduced penetration of PA into the pores of the substrate [21–25]. The average permeability of the membrane decreases with the thickness because of the increase in the mass transfer resistance with the increased membrane thickness, allowing less water to flow through. When the membrane thickness is too high, problems such as excessive pressure drop and cost arise.

The rejection of the SUS wastewater components and the overall rejection of organic species, as measured by TOC, is shown in Fig. 8a for the synthesized TFC at 100 μm thickness and the NF270 membranes. The results show that the in-house synthesized TFC membrane have enhanced selectivity towards the separation of HET and DTZ from the SUS feed. In addition, the synthesized TFC membrane exhibits better performance than the commercial membrane NF270 with respect to the rejection of both HET and MEA, as well as a lower rejection for DTZ. More specifically, for the synthesized TFC membrane, the rejection of

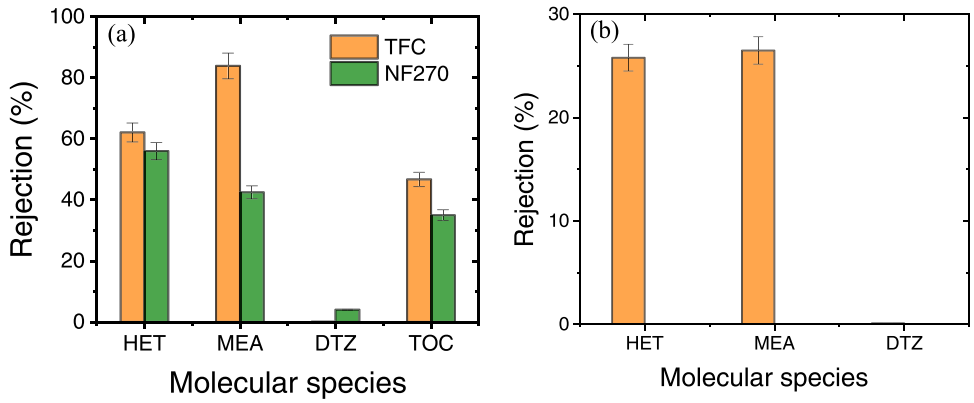

Fig. 8. a) Rejection of main compounds of the SUS solution using the NF270 and the synthesized TFC membrane; b) Rejection of HET, MEA and DTZ by the synthesized TFC membrane in single-solute solutions prepared with 1 g/L of HET, 10 g/L of MEA and 50 mg/L of DTZ in Milli-Q water at 40 °C, 100 μm membrane thickness, and 50% recovery.

HET and MEA was 62%, and 82%, respectively, while DTZ was not rejected at all. Meanwhile, for the NF270, the rejection of HET, MEA and DTZ was found to be approximately 56%, 43% and 4%, respectively. The main mechanisms that influence membrane separation are size exclusion, adsorption, electrostatic exclusion, and dielectric exclusion [45]. In this study, size exclusion and dielectric exclusion plays a major role for membrane separation. The highest rejection of HET may be related to the higher molecular size (219.28 Da) compared to the smaller size of DTZ (165.3 Da). Where the lowest rejection of DTZ can be explained by the larger dipole moment of DTZ (3.66 D) compared to the other two molecules, i.e., HET (1.31 D) and MEA (1.12 D). Other researchers have previously discussed that organic compounds with high dipole moment (>3 Debye) exhibit significantly lower rejection than expected based on a purely size exclusion mechanism [46,47]. Therefore, the molecule having a dipole moment is able to pass through the membrane structure and enter the pore more readily due to the attractive contact between its polar centers and immobilized charged groups on the membrane surface and this impact is stronger for molecules with cylindrical forms (high length to width ratio [12,48]. In addition, the n-octanol-water partition coefficient of DTZ (log K_{ow} equal to 0.9) indicates that DTZ is more hydrophobic than HET and MEA. Hydrophobic species have a tendency to adsorb on membrane surfaces and then pass through the membrane [49]. Overall, it is noteworthy to mention that the synthesized TFC membrane has twice the permeability of the NF270 while also exhibiting slightly improved rejection properties for HET and MEA and an improved separation selectivity of HET and DTZ. Moreover, the synthesized TFC had the highest TOC rejection of about 47 %, compared to 37 % for NF270.

To better understand how HET, MEA, and DTZ are separated from the SUS wastewater, three single-solute solutions containing 1 g/L of HET, 10 g/L of MEA and 50 mg/L of DTZ were prepared in Milli-Q water and filtered using the synthesized TFC membrane. Fig. 8b shows that the rejections of HET and MEA were approximately 26%, while the rejection of DTZ was close to zero. The very low rejection of DTZ and the substantially lower rejection of MEA, compared to the MEA rejection values measured when operating with the SUS, is very much in line with the literature findings on these molecular species utilizing the NF270 membrane [12]. Rejection data on single-solute solutions of HET were however not available in the literature. The results of this work show that also the rejection of HET, analogously to MEA, is substantially lower when operating on single-solute solutions, compared to the HET rejection measured when operating with the SUS. These results points towards a hypothesis that the high rejection of HET and MEA when operating on the SUS is caused by the interaction of HET and MEA via intermolecular hydrogen bonding and the formation of HET-MEA complexes of apparent larger molecular size. The hypothesis is based on research by Vorobyov et al., 2002) which demonstrated hydrogen bond formation in aqueous solutions of MEA [50]. Therefore, the interaction of the species and the size exclusion mechanism plays a key role in the rejection of HET, MEA, and DTZ from the SUS solution.

3.3. *Membrane fouling performance*

Fouling is a significant issue of membrane technology, which has negative implications such as a decrease of flux and the quality of filtered water. Severe fouling may require membrane replacement or chemical cleaning [51]. In this regard, an experiment was carried out to investigate the fouling propensity for the NF270 and the synthesized TFC membranes operating with the SUS over a longer period of operation (24 h). Fig. 9a shows that the permeability of the synthesized TFC membrane did not decrease and remained approximately constant at 6 ± 0.3 L/(m^2·h·bar) during its long-term operational stability. Fouling agents may easily adhere to the surface of hydrophobic membranes due to their hydrophobic nature itself. However, connecting to the hydrophilic surfaces of the membrane is difficult, and even if they could be linked, they could be rapidly dislodged from the surface by water penetration [52]. In addition, the TFC membrane shows good stability, where the feed and permeate TOC (Fig. S2) were also kept consistent within the range of 96–99 g/L and 71–80 g/L, respectively, indicating that the filtration was carried out in a continuous and high-quality manner. Furthermore, the TOC rejection (Fig. 9b) ranged from 40 % to 48 %, indicating that the permeate recirculation was completed effectively. The rejection of HET and MEA for both the membranes was almost constant during the long period of the filtration process. The NF270 had permeability of approximately 0.45 ± 0.05 L/(m^2·h·bar) and a TOC rejection of 37.5% when compared to synthesized TFC. This result shows that the synthesized TFC membrane exhibited much higher permeability (>10 times) compared to the commercial NF270 membrane.

4. Conclusions

This work presents the synthesis of a TFC polyamide membrane for the recovery of MEA-triazine (HET, unspent H_2S scavenger) from a wastewater produced in offshore oil and gas industry containing spent H_2S scavengers (DTZ). An investigation on the membrane performance, permeability, hydrophilicity, fouling, and the effect of the membrane thickness is presented. In comparison to the commercially available polyamide membrane NF270, tested in a previous work for this industrial application, the in-house synthesized TFC membranes of this work exhibit significant improvements in permeability 6 L/(m^2·h·bar) vs. 0.45 L/(m^2·h·bar), together with improved selectivity towards the separation HET/DTZ. More specifically, the rejection of HET and MEA with the in-house synthesized membrane was 62 % and 82 %, respectively,

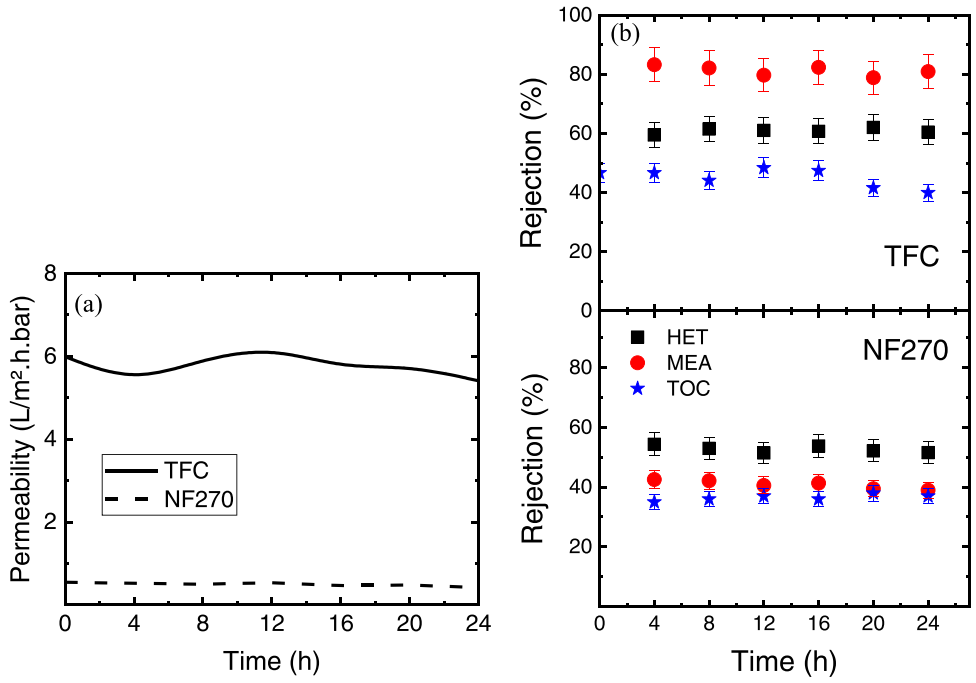

Fig. 9. Long term filtration test: a) Filtration permeability and b) HET, MEA, and TOC rejection using NF270 and synthesized TFC membrane at 40 °C, 100 μm membrane thickness, and 50 % recovery.

which represents an improvement from the 56 % for HET and 43 % for MEA observed with the NF270 membrane. In addition, the synthesized membrane in this work showed zero rejection for DTZ. The synthesized TFC membrane also showed higher TOC rejection (47 %) compared to the NF270 (37 %). The analysis of the effect of the membrane thickness showed an optimal value at 100 μm. The synthesized membrane also showed significant antifouling properties over 24 h of operation. Based on these findings, the low-cost TFC membrane synthesized in this work exhibits the ability to recover the unspent H_2S scavenger chemical MEA-triazine with high efficiency. It appears to be attractive for the design of a membrane separation process aimed at recovering the unspent scavenger and recycling it to the H_2S scavenging unit, thus reducing operating costs in production chemicals for the operator, as well as reducing the environmental impact factor related to the discharge of this chemical into the sea.

CRediT authorship contribution statement

Alaa Khalil: Conceptualization, Methodology, Software, Validation, Formal analysis, Investigation, Data curation, Writing – original draft, Writing – review & editing, Visualization. **Nikos Montesantos:** Conceptualization, Methodology, Validation, Investigation, Writing – review & editing. **Marco Maschietti:** Conceptualization, Methodology, Validation, Investigation, Writing – review & editing, Funding acquisition, Resources, Project administration. **Jens Muff:** Conceptualization, Methodology, Validation, Investigation, Writing – review & editing, Supervision, Funding acquisition, Resources, Project administration.

Declaration of Competing Interest

The authors declare that they have no known competing financial interests or personal relationships that could have appeared to influence the work reported in this paper.

Data Availability

The authors do not have permission to share data.

Acknowledgments

The work was financially supported by Danish Offshore Technology Centre as part of the work programme Produced Water Management. The authors would like to thank Jørgen Rentler Næumann (DTU Offshore, programme manager of the work programme Produced Water Management), Simon Ivar Andersen (DTU Offshore, research leader in Offshore Produced Water Management), Yanina D. Ivanova (DTU Offshore, production chemistry advisor), Ole Andersen (DTU Offshore, surface engineer advisor) for the continuous and insightful technical discussions during the execution of this work. The authors would like to thank also DTU offshore and Berit Wenzell for access and assistance in SEM images measurement.

Appendix A. Supporting information

Supplementary data associated with this article can be found in the online version at doi:10.1016/j.jece.2022.108735.

References

[1] F. Pouliquen, C. Blanc, E. Arretz, I. Labat, J. Tournier-Lasserve, A. Ladousse, J. Nougayrede, G. Savin, R. Ivaldi, M. Nicolas, J. Fialaire, R. Millischer, C. Azema, L. Espagno, H. Hemmer, J. Perrot, Hydrogen sulfide, in: Ullmann's Encyclopedia of Industrial Chemistry, Wiley-VCH Verlag GmbH Co. KGaA, Weinheim, 2012.
[2] N. Montesantos, M.N. Fini, J. Muff, M. Maschietti, Proof of concept of hydrothermal oxidation for treatment of triazine-based spent and unspent H2S scavengers from offshore oil and gas production, Chem. Eng. J. 427 (2022), 131020.
[3] J.J. Wylde, G.N. Taylor, K.S. Sorbie, W.N. Samaniego, Formation, Chemical Characterization, and Oxidative Dissolution of Amorphous Polymeric Dithiazine (apDTZ) during the Use of the H2S Scavenger Monoethanolamine-Triazine, Energy Fuels 34 (2020) 9923–9931.
[4] M.A. Kelland, Hydrogen Sulde Scavengers, in: Production Chemicals for the Oil and Gas Industry, CRC Press, 2014.
[5] G. Taylor, M. Smith-Gonzalez, J. Wylde, A.P. Oliveira, H2S Scavenger Development During the Oil and Gas Industry Search for an MEA Triazine Replacement in Hydrogen Sulfide Mitigation and Enhanced Monitoring Techniques Employed During Their Evaluation, in: SPE International Conference on Oilfield Chemistry, 2019.
[6] I. Romero, S. Kucheryavskiy, M. Maschietti, Experimental Study of the Aqueous Phase Reaction of Hydrogen Sulfide with MEA-Triazine Using In Situ Raman Spectroscopy, Ind. Eng. Chem. Res. 60 (2021) 15549–15557.

[7] R.G. Fiorot, J.W. de, M. Carneiro, The mechanism for H2S scavenging by 1,3,5-hexahydrotriazines explored by DFT, Tetrahedron 76 (2020), 131112.
[8] J.M. Bakke, J. Buhaug, J. Riha, Hydrolysis of 1,3,5-Tris(2-hydroxyethyl)hexahydro-s-triazine and Its Reaction with H2S, Ind. Eng. Chem. Res. 40 (2001) 6051–6054.
[9] ECHA., Monoethanolamine, in, March 29, 2021.
[10] L. Shu, N. Wang, C. Zhao, Y. Meng, S. Ji, J.-R. Li, Facile Fabrication of High Performance Nanofiltration Membranes by Using Molecular Coordination Complexes as Pore-Forming Agents, ACS Sustain. Chem. Eng. 7 (2019) 2728–2738.
[11] M. Nikbakht Fini, H.T. Madsen, J. Muff, The effect of water matrix, feed concentration and recovery on the rejection of pesticides using NF/RO membranes in water treatment, Sep. Purif. Technol. 215 (2019) 521–527.
[12] M. Nikbakht Fini, N. Montesantos, M. Maschietti, J. Muff, Performance evaluation of membrane filtration for treatment of H2S scavenging wastewater from offshore oil and gas production, Sep. Purif. Technol. 277 (2021), 119641.
[13] Y.S. Khoo, W.J. Lau, Y.Y. Liang, M. Karaman, M. Gürsoy, A.F. Ismail, Eco-friendly surface modification approach to develop thin film nanocomposite membrane with improved desalination and antifouling properties, J. Adv. Res. 36 (2022) 39–49.
[14] M. Alberto, R. Bhavsar, J.M. Luque-Alled, E. Prestat, L. Gao, P.M. Budd, A. Vijayaraghavan, G. Szekely, S.M. Holmes, P. Gorgojo, Study on the formation of thin film nanocomposite (TFN) membranes of polymers of intrinsic microporosity and graphene-like fillers: Effect of lateral flake size and chemical functionalization, J. Membr. Sci. 565 (2018) 390–401.
[15] L. Shen, R. Cheng, M. Yi, W.-S. Hung, S. Japip, L. Tian, X. Zhang, S. Jiang, S. Li, Y. Wang, Polyamide-based membranes with structural homogeneity for ultrafast molecular sieving, Nature, Communications 13 (2022) 500.
[16] M.H. Tajuddin, N. Yusof, N. Fajrina, W.N.W. Salleh, A.F. Ismail, J. Jaafar, F. Aziz, Tailoring the properties of polyamide thin film membrane with layered double hydroxide nanoclay for enhancement in water separation, Curr. Appl. Phys. 34 (2022) 36–40.
[17] Z.-M. Zhan, X. Zhang, Y.-X. Fang, Y.-J. Tang, K.-K. Zhu, X.-H. Ma, Z.-L. Xu, Polyamide Nanofiltration Membranes with Enhanced Desalination and Antifouling Performance Enabled by Surface Grafting Polyquaternium-7, Ind. Eng. Chem. Res. 60 (2021) 14297–14306.
[18] S.C. Mamah, P.S. Goh, A.F. Ismail, N.D. Suzaimi, L.T. Yogarathinam, Y.O. Raji, T. H. El-badawy, Recent development in modification of polysulfone membrane for water treatment application, J. Water Process Eng. 40 (2021), 101835.
[19] N. Arahman, A. Fahrina, S. Amalia, R. Sunarya, S. Mulyati, Effect of PVP on the characteristic of modified membranes made from waste PET bottles for humic acid removal, F1000Res 6 (2017), 668-668.
[20] T.T.V. Tran, S.R. Kumar, C.H. Nguyen, J.W. Lee, H.-A. Tsai, C.-H. Hsieh, S.J. Lue, High-permeability graphene oxide and poly(vinyl pyrrolidone) blended poly (vinylidene fluoride) membranes: Roles of additives and their cumulative effects, J. Membr. Sci. 619 (2021), 118773.
[21] X. Zhang, M. Wei, F. Xu, Y. Wang, Thickness-dependent ion rejection in nanopores, J. Membr. Sci. 601 (2020), 117899.
[22] F. Liu, L. Wang, D. Li, Q. Liu, B. Deng, A review: the effect of the microporous support during interfacial polymerization on the morphology and performances of a thin film composite membrane for liquid purification, RSC Adv. 9 (2019) 35417–35428.
[23] Y. Liu, X. Chen, High permeability and salt rejection reverse osmosis by a zeolite nano-membrane, Phys. Chem. Chem. Phys. 15 (2013) 6817–6824.
[24] B. Khorshidi, T. Thundat, B.A. Fleck, M. Sadrzadeh, A Novel Approach Toward Fabrication of High Performance Thin Film Composite Polyamide Membranes, Sci. Rep. 6 (2016) 22069.
[25] P. Veerababu, B.B. Vyas, P.S. Singh, P. Ray, Limiting thickness of polyamide–polysulfone thin-film-composite nanofiltration membrane, Desalination 346 (2014) 19–29.
[26] M. Nikbakht Fini, J. Zhu, B. Van der Bruggen, H.T. Madsen, J. Muff, Preparation, characterization and scaling propensity study of a dopamine incorporated RO/FO TFC membrane for pesticide removal, J. Membr. Sci. 612 (2020), 118458.
[27] J.T. Arena, B. McCloskey, B.D. Freeman, J.R. McCutcheon, Surface modification of thin film composite membrane support layers with polydopamine: Enabling use of reverse osmosis membranes in pressure retarded osmosis, J. Membr. Sci. 375 (2011) 55–62.
[28] F. Samperi, C. Puglisi, R. Alicata, G. Montaudo, Thermal degradation of poly (ethylene terephthalate) at the processing temperature, Polym. Degrad. Stab. 83 (2004) 3–10.
[29] D. Nasirian, I. Salahshoori, M. Sadeghi, N. Rashidi, M. Hassanzadeganroudsari, Investigation of the gas permeability properties from polysulfone/polyethylene glycol composite membrane, Polym. Bull. 77 (2020) 5529–5552.
[30] S. Elhady, M. Bassyouni, R.A. Mansour, M.H. Elzahar, S. Abdel-Hamid, Y. Elhenawy, M.Y. Saleh, Oily Wastewater Treatment Using Polyamide Thin Film Composite Membrane Technology, Membranes 10 (2020) 84.
[31] M.H.Pd.S. Ana Paula dos Santos Pereira, Édio Pereira Lima Júnior, Andersan dos Santos Paula, Flávio James Tommasini Processing and Characterization of PET Composites Reinforced With Geopolymer Concrete Waste, Mat. Res. Vol. 20 (suppl 2) (2017) 411–420.
[32] S. Belfer, R. Fainchtain, Y. Purinson, O. Kedem, Surface characterization by FTIR-ATR spectroscopy of polyethersulfone membranes-unmodified, modified and protein fouled, J. Membr. Sci. 172 (2000) 113–124.
[33] J. Zheng, Y. Li, D. Xu, R. Zhao, Y. Liu, G. Li, Q. Gao, X. Zhang, A. Volodine, B. Van der Bruggen, Facile fabrication of a positively charged nanofiltration membrane for heavy metal and dye removal, Sep. Purif. Technol. 282 (2022), 120155.
[34] Y. Wang, Z. Fang, S. Zhao, D. Ng, J. Zhang, Z. Xie, Dopamine incorporating forward osmosis membranes with enhanced selectivity and antifouling properties, RSC Adv. 8 (2018) 22469–22481.
[35] A. Yahia Cherif, O. Arous, N. Mameri, J. Zhu, A. Ammi Said, I. Vankelecom, K. Simoens, K. Bernaerts, B. Van der Bruggen, Fabrication and characterization of novel antimicrobial thin film nano-composite membranes based on copper nanoparticles, J. Chem. Technol. Biotechnol. 93 (2018) 2737–2747.
[36] M.H. Tajuddin, N. Yusof, I. Wan Azelee, W.N. Wan Salleh, A.F. Ismail, J. Jaafar, F. Aziz, K. Nagai, N.F. Razali, Development of Copper-Aluminum Layered Double Hydroxide in Thin Film Nanocomposite Nanofiltration Membrane for Water Purification Process, Front. Chem. 7 (2019).
[37] M.B. El-Arnaouty, A.M. Abdel Ghaffar, M. Eid, M.E. Aboulfotouh, N.H. Taher, E.-S. Soliman, Nano-modification of polyamide thin film composite reverse osmosis membranes by radiation grafting, J. Radiat. Res. Appl. Sci. 11 (2018) 204–216.
[38] J.C. Farias-Aguilar, M.J. Ramírez-Moreno, L. Téllez-Jurado, H. Balmori-Ramírez, Low pressure and low temperature synthesis of polyamide-6 (PA6) using Na0 as catalyst, Mater. Lett. 136 (2014) 388–392.
[39] S. Agrawal, N. Ingle, U. Maity, R.V. Jasra, P. Munshi, Effect of Aqueous HCl with Dissolved Chlorine on Certain Corrosion-Resistant Polymers, ACS Omega 3 (2018) 6692–6702.
[40] T. Le, E. Jamshidi, M. Beidaghi, M.R. Esfahani, Functionalized-MXene Thin-Film Nanocomposite Hollow Fiber Membranes for Enhanced PFAS Removal from Water, ACS Appl. Mater. Interfaces 14 (2022) 25397–25408.
[41] Y.A. Stetsiv, M.M. Yatsyshyn, D. Nykypanchuk, S.A. Korniy, I. Saldan, O. V. Reshetnyak, T.J. Bednarchuk, Characterization of polyaniline thin films prepared on polyethylene terephthalate substrate, Polym. Bull. 78 (2021) 6251–6265.
[42] R. Modi, R. Mehta, H. Brahmbhatt, A. Bhattacharya, Tailor Made Thin Film Composite Membranes: Potentiality Towards Removal of Hydroquinone from Water, J. Polym. Environ. 25 (2017) 1140–1146.
[43] J. Ren, J.R. McCutcheon, A new commercial thin film composite membrane for forward osmosis, Desalination 343 (2014) 187–193.
[44] M.Q. Seah, W.J. Lau, P.S. Goh, H.-H. Tseng, R.A. Wahab, A.F. Ismail, Progress of Interfacial Polymerization Techniques for Polyamide Thin Film (Nano)Composite Membrane Fabrication: A Comprehensive Review, Polymers 12 (2020).
[45] E. Mancini, P. Ramin, P. Styrbæck, C. Bjergholt, S. Soheil Mansouri, K.V. Gernaey, J. Luo, M. Pinelo, Separation of succinic acid from fermentation broth: Dielectric exclusion, Donnan effect and diffusion as the most influential mass transfer mechanisms, Sep. Purif. Technol. 281 (2022), 119904.
[46] A.M. Comerton, R.C. Andrews, D.M. Bagley, P. Yang, Membrane adsorption of endocrine disrupting compounds and pharmaceutically active compounds, J. Membr. Sci. 303 (2007) 267–277.
[47] S. Kim, K.H. Chu, Y.A.J. Al-Hamadani, C.M. Park, M. Jang, D.-H. Kim, M. Yu, J. Heo, Y. Yoon, Removal of contaminants of emerging concern by membranes in water and wastewater: A review, Chem. Eng. J. 335 (2018) 896–914.
[48] L.D. Nghiem, A.I. Schäfer, M. Elimelech, Pharmaceutical Retention Mechanisms by Nanofiltration Membranes, Environ. Sci. Technol. 39 (2005) 7698–7705.
[49] Y. Kiso, Y. Sugiura, T. Kitao, K. Nishimura, Effects of hydrophobicity and molecular size on rejection of aromatic pesticides with nanofiltration membranes, J. Membr. Sci. 192 (2001) 1–10.
[50] I. Vorobyov, M.C. Yappert, D.B. DuPré, Hydrogen Bonding in Monomers and Dimers of 2-Aminoethanol, The, J. Phys. Chem. A 106 (2002) 668–679.
[51] H. Rezania, V. Vatanpour, Preparation and modification of thin film composite membrane using a bulky dianhydride monomer, J. Appl. Polym. Sci. 138 (2021) 51389.
[52] H. Li, W. Shi, Q. Du, R. Zhou, H. Zhang, X. Qin, Improved separation and antifouling properties of thin-film composite nanofiltration membrane by the incorporation of cGO, Appl. Surf. Sci. 407 (2017) 260–275.